LAWRENCE
LIVERMORE
NATIONAL
LABORATORY

LLNL-JRNL-420428

Extended model for Richtmyer-Meshkov mix

K. O. Mikaelian

November 19, 2009

Physics of Fluids

Disclaimer

Extended model for Richtmyer-Meshkov mix

Karnig O. Mikaelian
Lawrence Livermore National Laboratory
Livermore, California 94551

Abstract

We examine four Richtmyer-Meshkov (RM) experiments on shock-generated turbulent mix and find them to be in good agreement with our earlier simple model in which the growth rate $\dot{h}$ of the mixing layer following a shock or reshock is constant and given by $2\alpha A\Delta v$, independent of initial conditions h_0. Here A is the Atwood number $(\rho_B - \rho_A)/(\rho_B + \rho_A)$, $\rho_{A,B}$ are the densities of the two fluids, Δv is the jump in velocity induced by the shock or reshock, and α is the constant measured in Rayleigh-Taylor (RT) experiments: $\alpha^{bubble} \approx 0.05-0.07$, $\alpha^{spike} \approx (1.8-2.5)\alpha^{bubble}$ for $A \approx 0.7-1.0$. In the extended model the growth rate begins to decay after a time t^*, when $h = h^*$, slowing down from $h = h_0 + 2\alpha A\Delta vt$ to $h \sim t^{\theta}$ behavior, with $\theta^{bubble} \approx 0.25$ and $\theta^{spike} \approx 0.36$ for $A \approx 0.7$. We ascribe this change-over to loss of memory of the *direction* of the shock or reshock, signaling transition from highly directional to isotropic turbulence. In the simplest extension of the model h^*/h_0 is independent of Δv and depends only on A. We find that $h^*/h_0 \approx 2.5-3.5$ for $A \approx 0.7-1.0$.

I. INTRODUCTION

Hydrodynamic instabilities between two fluids and in particular Rayleigh-Taylor[1,2] (RT) and Richtmyer-Meshkov[3,4] (RM) instabilities acquired new importance since the proposal[5] to use inertial confinement fusion to achieve thermonuclear burn.[6] In astrophysics they challenge our ability to explain certain phenomena such as supernova explosions.[7] These hydrodynamic instabilities cause the two fluids to interpenetrate and mix. Experimental, numerical and theoretical efforts continue to shed light on these complex, yet basic processes.[8]

The original works on RT[1,2] and RM[3,4] instabilities were naturally limited to the single-scale linear regime. For RT, perturbations of amplitude η and wavelength λ grow at the interface between two fluids of densities ρ_A and ρ_B under a constant acceleration $\vec{g}$ directed from A to B with $\rho_A < \rho_B$. For RM, perturbations grow if a shock passes from A to B or B to A. In the latter case the growth is preceded by a phase reversal. The linear regime for both instabilities is limited to $\eta << \lambda$.

As the amplitude grows it enters the nonlinear regime $\eta \geq \lambda$ and slows down but continues to grow. There is a vast and growing literature on nonlinear evolution that we forgo except to mention that due to the difficulty of nonlinear equations several models have been developed, of which we cite only Layzer's original work.[9] Its descendants are too numerous to report and not quite germane to the subject at hand which is turbulent mix, a topic even more challenging: multi-wavelength initial perturbations, shocked or accelerated, evolving into turbulence. There are no expectations for an exact, first-principles description of turbulent mix anytime soon and therefore the development of models is even more requisite.

In Sec. II we review briefly the experiments on RT and RM mix, with emphasis on the latter. In Sec. III we extend our earlier model for RM mix and apply it to recent experiments. Conclusions, future work, and suggestions for new experiments are presented in Sec. IV.

II. RT & RM EXPERIMENTS

We believe the first experiments on RT mix were those of Read[10] guided and supported by the numerical simulations of Youngs.[11] The mix is initiated by a multitude of wavelengths some having amplitudes in the linear $\eta_i < \lambda_i$ and others in the nonlinear $\eta_i > \lambda_i$ regime, a combination that we call "random" for short. The resulting evolution, a very brief time after the start of the acceleration, was strikingly simple:

$$h = \alpha A g t^2, \tag{1}$$

where h is the mixing width, α a constant, and A is the Atwood number $(\rho_B - \rho_A)/(\rho_B + \rho_A)$. In our notation h stands for h^b or h^s and α for the corresponding α^b or α^s, with h^b (h^s) referring to the mixing layer width on the bubble (spike) side, i.e., the penetration depth of the light (heavy) fluid into the other. The experiments[10] were driven by rockets and hence are often referred to as "rocket-rig" experiments. Initial conditions $h_0 \equiv h(t = 0)$ were not measured except to note that they were small and, as is clear from Eq. (1), they did not influence the growth of $h(t)$, a fact often referred to as "loss of memory of initial conditions." Only h^b was measured with $\alpha^b \approx 0.07$ constant for a large range of Atwood numbers.

Several subsequent experiments, of which we mention only a couple, confirm the above picture. "Water channel"[12] experiments reported $\alpha^b \approx \alpha^s \approx 0.07$. These were low-$A$ experiments and therefore it is expected that $h^b \approx h^s$. "LEM" (Linear Electric Motor)

experiments[13] reported $\alpha^b \approx 0.05$ and $\alpha^s \approx \alpha^b[(1+A)/(1-A)]^{0.33} = \alpha^b[\rho_B/\rho_A]^{0.33}$ for $A \le 0.8$. We know of no experiment reporting any large effect of initial conditions on the RT mixing rate and in fact efforts to reduce mixing by reducing h_0 (smoother initial surfaces) have been largely unsuccessful, and the principle of "independence from initial conditions" appears well established. There are models predicting smaller α's for h_0 below a threshold,[14] but apparently this threshold is difficult to achieve experimentally.

Turning to RM, the first model proposed[15]

$$h = 2\alpha A \Delta v t , \tag{2}$$

thus maintaining the principle of "independence from initial conditions" and providing a complete prediction for the mixing width: α is the same constant as measured previously in RT experiments and Δv is the jump in the velocity of the interface induced by the shock. An initial-mix-width h_0 can appear as an additive constant in Eqs. (1) and (2) for consistency, but for now we take $h_0 << h$.

The purpose of this study is to compare Eq. (2) and its extension (see next section) with four RM experiments. First came the experiments of Vetter and Sturtevant[16] (VS) in a large shock tube. Next were the experiments of Erez *et al*[17] (ESOELSB) in a smaller shock tube. The same shock tube was used in an extended set of experiments reported recently by Leinov *et al*[18] (LMELBSS). These were all gas/gas experiments, in contrast to a gas/liquid experiment in an even smaller shock tube reported recently by Shi *et al*[19] (SZDJ). We shall discuss three of the experiments (VS, ESOELSB, and SZDJ) briefly, and examine the fourth one, LMELBSS, in some detail.

All gas/gas experiments use air and SF_6 as the two gases in a horizontal shock tube and rely on a membrane to separate the gases initially. In addition, VS used a pair of thin-wire-grids and placed the membrane in 3 different locations: i) Before, i.e., upstream side, ii) Between, or iii) After, i.e., downstream side of the grids. Once such a composite interface was shocked each configuration gave a different evolution. Upon reshock, however, the growth rate was found to be practically the same in all three configurations and in good agreement, within 23%, with Eq. (2) (a reshock occurs when the initial shock, transmitted from air into SF_6, reflects off the endwall and returns to reshock the air/SF_6 interface). Thus what was a liability (membrane and wire meshes affecting initial growth) was turned into an asset because the reflected shock met different conditions yet produced essentially the same $\dot{h}$, confirming the principle of "independence from initial conditions" mentioned above. VS measured only the total mixing width $h^t \equiv h^b + h^s \equiv h^{b+s}$ (this is true of ESOELSB and LMELBSS also), and $\dot{h}^{b+s} = 2(\alpha^b + \alpha^s) A \Delta v$, where A refers to the postreshock Atwood number. VS assumed $\alpha^b = \alpha^s = 0.07$ and hence the coefficient 0.28 in Eq. (2) of Ref. 16. To vary Δv, experiments with different shock Mach numbers M_s were performed using a long, 122 cm test section for the low-M_s and a short, 61 cm test-section for the high-M_s experiments. The change in length was needed to keep the reshocked mixing layer within their diagnostic window.[16] Higher Mach numbers showed better agreement with Eq. (2).

ESOELSB experiments used a "thin" (0.5 μm) or a "thick" (2.0 μm) membrane to separate the gases initially. Again, the mixing width after the first shock depended on the type of membrane used, but the growth after reshock appeared to be linear in time and, perhaps more

importantly, approximately independent of which membrane was used and how large was the mixing width just before reshock. No comparison with Eq. (2) was made.

The experiment reported by SZDJ[19] is performed in a vertical, downward-firing shock tube needing no membrane between the air, in which the shock is generated, and the water. Mach numbers ranged from 1.2 to 1.7. After the passage of the shock the air/water mixing widths were found to increase linearly with time and in good agreement with Eq. (2). The authors report[19] $\alpha^b = 0.052$ and $\alpha^s = 2.5\alpha^b = 0.13$. The high value of α^s is consistent with the higher value of A: $A \approx 1$ for air/water compared with $A \approx 0.7$ for air/SF_6. We do not analyze further the SZDJ experiments, but interpret their result as another possible confirmation of Eq. (2) – No other gas/liquid experiments of this type have been reported.

Finally, we consider in some detail the recently published LMELBSS experiments[18] that were conducted in the same shock tube as ESOELSB and used only one type (thin) membrane. Since evolution after first shock was known to depend on the membrane, the focus was again on the reshock. Three different methods were used to test Eq. (2).

The first method was the same one used in VS: Scan over Mach numbers. As the Mach number M_s of the incident shock is increased, Δv increases while A changes much less. For example, from our one-dimensional (1D) CALE[20] simulations (see below) we find that as M_s increases from 1.15 to 1.33 Δv more than doubles from 72 m/s to 149 m/s while the postreshock A increases only from 0.71 to 0.74.

Method 2 used in LMELBSS was a simple yet important variant of VS: Change the length of the test section but *keep* M_s *the same*. Vetter and Sturtevant had changed both the length of their test section and M_s simultaneously to accommodate their diagnostics; Leinov *et*

al. changed only the length to delay the arrival of the reshock at the same M_s, thus producing a more evolved interface to be reshocked with essentially the same Δv – in short, to vary the initial conditions at reshock time and see if a more evolved interface underwent more or less growth upon reshock with the same Δv.

In this second method the length was varied from 80 mm to 235 mm stepping through intermediate values, resulting in ~56% change in h_-, the mixing width just before reshock. The postreshock growth, however, did not change much, less than about 12%, in agreement with Eq. (2) and ESOELSB who had induced an even more modest change by varying the membrane.

The third and most innovative method used by LMELBSS was to use what we call "shock absorbers" instead of a rigid end wall, keeping everything else the same. A foam with no covering (least reflective), or with a cardboard covering (intermediate), or with an aluminum covering (more reflective) was used and the results compared with the most reflective case (rigid wall). The same M_s (1.20) and length (80 mm) was used throughout this scan. The first shock being the same in all cases, the shock absorbers reduce only the strength of the reflected shock, $\Delta v_{\text{reshock}}$ decreases, and the interface is (slightly) more evolved (weaker reshocks arrive slightly later). The experimentally measured Δv's ranged from a low of 36.3 ± 6.0 m/s using foam with no covering to a high of 96.4 ± 5.0 m/s with the rigid wall. The mixing widths were again found to be well correlated with Δv.

Clever as this technique is, it is a passive one serving only to weaken the reshock. We would like to advocate an active technique where the end wall is replaced not by a shock absorber but by a second high pressure chamber that is burst at an appropriate time to *increase* the reshock.

The experimental total growth rates $\dot{h}^{b+s}$ were compared[18] with $2(\alpha^b + \alpha^s)A\Delta v$ using $A = 0.712$. From the LEM experiments[13] $\alpha^s \approx \alpha^b[(1+A)/(1-A)]^{0.33} \approx 1.8\alpha^b$, hence $2(\alpha^b + \alpha^s) \approx 5.6\alpha^b \approx 0.28 - 0.39$ for $\alpha^b = 0.05 - 0.07$. The data (last figure in LMELBSS) appears to favor the upper end, and scaling with Δv appears reasonable (Tables 1-3 in Ref. 18). For brevity in this paper we adopt the intermediate value $\alpha^b = 0.06$ for which $2(\alpha^b + \alpha^s) \approx 5.6\alpha^b \approx 0.34$ for $A = 0.712$.

Although the experiments focused on the reshock, it is instructive to observe the behavior of the mixing width before and after, as ample data is presented in LMELBSS. We mentioned that the growth immediately following the first shock is "corrupted" by the membrane; however, the subsequent evolution shows an essentially decaying $\dot{h}$ until the reshock arrives. In fact the scan through successively longer and longer test sections (method 2) is also a record of how $h(t)$ evolves with time after the first shock – See Table 1 in LMELBSS.

After reshock the newly acquired and large value of $\dot{h}$ appears to remain constant for some time before it also begins to decay, particularly in the long-test-section experiments. In the short sections a third wave, a rarefaction, is captured in the diagnostic but the data stop too short a time thereafter to draw any conclusions. We shall not consider the third signal in this paper.

III. EXTENDED MODEL AND AIR/SF_6 EXPERIMENTS

We shall focus on the experiments of Leinov *et al.*[18] to extend the model based on Eq. (2). This is necessary if one wishes to account for the experiments from $t = 0$ when the first shock strikes the air/SF_6 interface and not just after reshock for which Eq. (2) appears to be adequate.[16,18,19] Keeping in mind that the first shock may be "corrupted" by the presence of the

membrane we shall, nevertheless, apply the model starting from $t=0$ as was done in SZDJ. One would be clearly justified in introducing a multiplier in Eq. (2) to account for the membrane effect, but we shall forgo such an approach and use Eq. (2) as is. Instead, we believe it is important to capture the subsequent *decay* of the growth rate from its constant value $2\alpha A\Delta \mathrm{v}$ to essentially zero. Thus the model we propose is to use Eq. (2) until a time, call it t^*, when the mixing width changes from Eq. (2) to

$$h = h^*\left(1+\frac{\dot{h}^*}{\theta h^*}(t-t^*)\right)^{\theta}, \tag{3}$$

where $h^* = h(t^*)$ and $\dot{h}^* = \dot{h}(t^*)$, ensuring continuity of h and $\dot{h}$. Equation (3) is the solution of the so-called drag equation,

$$\frac{d^2h}{dt^2} = -c_d\dot{h}^2/h = (1-1/\theta)\dot{h}^2/h. \tag{4}$$

For $t >> t^*$ it has the form t^{θ} predicted by bubble-merger models[21,22] and has been often used to describe h after the acceleration g has been turned off (see, e.g., Ref. 13 and references therein). Solutions to the more general buoyancy-drag equation can be found in Ref. 23. From LEM experiments[13] we take $\theta^b \approx 0.25$ and $\theta^s \approx \theta^b[(1+A)/(1-A)]^{0.21}$, which gives $\theta^s \approx 0.36$ for $A = 0.712$. We should caution the reader that all the "constants" used in this paper (α^b, α^s, θ^b, and θ^s) have some experimental uncertainties associated with them.[10,12,13]

If the decay, Eq. (3), follows RT growth then $\dot{h}^*/h^* = 2\alpha A g t^*/\alpha A g(t^*)^2 = 2/t^*$. If it follows RM growth then $\dot{h}^*/h^* = 2\alpha A\Delta \mathrm{v}/2\alpha A\Delta \mathrm{v} t^* = 1/t^*$, and Eq. (3) becomes

$$h = h^*\left(1+\frac{2}{\theta}(t/t^*-1)\right)^{\theta}, \text{ following RT} \quad , \tag{5a}$$

$$h = h^*\left(1+\frac{1}{\theta}(t/t^*-1)\right)^{\theta}, \text{ following RM.} \qquad (5b)$$

Clearly, one needs only one parameter, either the time t^* or the mixing width h^* when decay begins, because given one the other is determined via $h^*/t^* = 2\alpha A\Delta v$ for RM. We continue to take $h_0 \approx 0$ and discuss a finite h_0, which must be added to Eqs. (1) and (2), in Sec. IV.

In this model it is difficult to maintain the principle that "RM remembers its initial conditions" as is often claimed. If $h \sim \Delta v t$ independent of initial conditions how can its subsequent evolution depend on it? A possible answer may be "If t^* depends on h_0." At present there is no theoretical, numerical or experimental data to judge the validity of such a connection between t^* and h_0, which we will make in Sec. IV.

The two-regime methodology advocated in this model is similar to Fermi's model for the evolution of a single-scale RT perturbation $\eta(t)$ as quoted by Layzer.[9] Details can be found in Ref. 24 where a similar, but slightly different approach to nonlinear RT and RM instabilities was proposed. Let us only point out that in the case of the single-scale RT or RM problem t^* is indeed determined by η_0, the initial amplitude. In Fermi's case continuity of $\dot{\eta}$ was the link between t^* and η_0 (see Ref. 24). Here, however, t^* cannot be determined in this fashion because Eq. (3) satisfies continuity of h and $\dot{h}$ for *any* t^*.

A principle that may help identify t^* will be mentioned at the end. Here we treat it as a free variable and find that the experiments already constitute a nontrivial test of the model. The question is: Can one, with a *single* parameter t^*, match the experimental mixing widths in the successively longer and longer test sections?

To model the experiments of Leinov *et al.*[18] we have used the following input parameters: $\rho_{SF_6}/\rho_{air} = 5.1$, $\gamma_{SF_6} = 1.09$, $\gamma_{air} = 1.40$. Given the Mach number M_s of the incoming shock, the Rankine-Hugoniot relations determine the postshock Atwood number and the velocity v_1 of the air/SF_6 interface. This is also $\Delta\mathrm{v}$ for the first shock. For the reshock, we need the length L of the SF_6 test section and the nature of the endwall. The shock that is transmitted into the SF_6 reflects fully from a rigid wall (the SF_6 comes to rest next to the wall), but only partially if a shock absorber is present. In all cases, however, the reflected shock meets the interface, still moving at velocity v_1, and reshocks it so it now moves at velocity v_2, and has a slightly different $A_{after\ reshock}$. The reshock time is proportional to L, and $\Delta\mathrm{v} = |\mathrm{v}_2 - \mathrm{v}_1|$ for the reshock. We found it useful to run 1D CALE problems for several experiments and check the results against standard Rankine-Hugoniot solutions.[25] We adopt the units of LMELBSS: millimeters for distance, milliseconds for time, and meter/second for velocity. Unlike LMELBSS, who took $t = 0$ to coincide with the reshock, we take $t = 0$ to be the time the first shock strikes the interface.

An example with $M_s = 1.20$, $L = 80$ mm will clarify. We find $\mathrm{v}_1 = 69.1$ m/s, $A_{after\ shock} = 0.70$. For a rigid endwall we find $\mathrm{v}_2 = -24.8$ m/s, $A_{after\ reshock} = 0.72$, hence $\Delta\mathrm{v} = 93.9$ m/s for the reshock, which arrives at $t \approx 0.72$ ms. Taking $t^* = 0.1$ ms, the evolution of the total mixing width h^{b+s} is plotted in Fig. 1 as a function of time. We have used Eq. (2) for $t \le t^*$ and switched to Eq. (5b) for $t \ge t^*$. In the same figure we show the evolution for the longest, $L = 235$ mm experiment. Note that while L was increased almost 3-fold and hence reshock occurred 3 times later (~2.15 ms), the mixing width h_- before reshock has increased from ~4.2 mm to ~6.2 mm only. The postreshock growth rate $\dot{h}$ is the same, $2(\alpha^b + \alpha^s)A\Delta\mathrm{v} \sim 22.9$ m/s in

both cases. Experimentally (Table 1 in Ref. 18) the growth rate ranged between 21.8 ± 1 and 24.3 ± 1 m/s for L between 80 and 235 mm and there was no correlation between $\dot{h}$ and h_{-}.[18]

The nontrivial test for t^* hinted at earlier is the evolution of h^{b+s} between t^* and reshock time. For a fixed M_s, as the length L of the test section is increased in steps from 80 mm to 235 mm one must, for consistency, use the same t^* for the first shock, as we did in Fig. 1. This period of evolution is similar to Fig. 7 of LMELBSS, its horizontal axis now interpreted as time. In short, Eq. (3) appears to agree well with Fig. 7 of LMELBSS after converting its x-axis (mm) to time (ms).

In Fig. 1 we also show h^{b+s} for the stronger, $M_s = 1.33$ shock, done only in the short ($L = 80$ mm) test section with a rigid endwall. We find $\mathrm{v}_1 = 108.6$ m/s and $A_{after\ shock} = 0.72$, therefore the growth rate after the first shock is ~108.6/69.1 or about 1.57 times larger than the $M_s = 1.20$ case. The ratio goes up to 1.64 after including Atwood number effects appearing in Eq. (2) and in α^s. We have not changed t^* (0.1 ms, though it is likely to depend on M_s - see below), and again used Eqs. (3) or (5b) from t^* until reshock which now occurs at 0.57 ms. After reshock $\mathrm{v}_2 = -40.0$ m/s and $A_{after\ reshock} = 0.74$, therefore the postreshock growth is ~148.6/93.9 or about 1.58 times larger than the weaker, $M_s = 1.20$ case. Including A-effects, that ratio goes up to 1.65. Clearly, $\Delta \mathrm{v}$ is the major player controlling h.

To compare our postreshock growth rates with experiment (Table 2 in Ref. 18), we find $\dot{h}^{b+s} \approx 38$ m/s for $\Delta \mathrm{v} = 149$ m/s, compared with $\dot{h}^{b+s} \approx 34.6 \pm 3$ m/s for $\Delta \mathrm{v} = 145.6 \pm 10$ m/s experimentally. We should add that the agreement is somewhat poorer (see below) for the weaker shocks.

As mentioned earlier we terminate our calculation when a third signal hits the interface in the short-section experiments. In the long ($L = 235$ mm) section, however, one observes a decay ~0.4 ms after reshock. We capture this phase by using Eq. (3) a second time starting at $t \approx 2.55$ ms in Fig. 1.

We now turn to the experiments with shock absorbers, all done at $M_s = 1.20$ in the short, 80 mm-long test section, and therefore all having $\mathrm{v}_1 = 69.1$ m/s, $A_{after\ shock} = 0.70$. The effect of a shock absorber is to reduce $\Delta \mathrm{v}_{\mathrm{reshock}}$. Those are listed in Table 3 of Ref. 18. From this table we conclude that, in increasing rigidity, $\mathrm{v}_2 = 32.8 \pm 6$, 23.7 ± 6, and -3.9 ± 6 m/s for the elastomeric foam (EF), elastomeric foam & cardboard (EF&C), and elastomeric foam & aluminum plate (EF&AP) endwalls, respectively, compared with -24.8 m/s for the fully rigid wall. Although the $\Delta \mathrm{v}$'s listed in Table 3 of Ref. 18 are (almost) sufficient to construct the corresponding growth rates from Eq. (2) ("almost" because one also needs the Atwood numbers), we found it useful again to model each absorber as a third fluid, call it C, placed behind the 80 mm-long SF_6 and whose density ρ_{C} is chosen to produce the required strength in the reflected shock, a method we had advocated recently.[26] γ_{C} having a much weaker effect on the reflected shock we kept it at 1.09 while varying only ρ_{C}. There is a one-to-one correspondence between ρ_{C} and the strength of the reflected shock, and this is a well-posed and simple exercise matching ρ_{C} to the required v_2. We found that by choosing $\rho_{\mathrm{C}} / \rho_{SF_6} \approx 3$, 5, and 40, one closely matches the v_2's listed for the three shock absorbers EF, EF&C, and EF&AP, respectively, compared with $\rho_{\mathrm{C}} / \rho_{SF_6} = \infty$ for the rigid wall. The corresponding postreshock Atwood numbers $A_{after\ reshock}$ are 0.709, 0.711, and 0.716, compared with 0.720 for the rigid case, again a minor change.

Fig. 2(a) displays the interface velocities as functions of time for the four cases [rigid endwall included for comparison]. Note that the weaker reshocks EF and EF&C cannot reverse the direction of motion, i.e., leave $v_2 > 0$ (curves labeled A and B), while EF&AP (curve C) almost brings the interface to rest, meaning $v_2 \sim 0$. The diagnostic advantages of $v_2 = 0$ are obvious: The turbulent mixing zone is at rest and grows wider with time. In addition, $|\Delta v|_{reshock} = |\Delta v|_{shock}$ and therefore $\dot{h}|_{reshock} = \dot{h}|_{shock}$, the only difference being essentially the sign of A and the mix width h_- and its rate of change $\dot{h}_-$ just before reshock being different from those of the shock. In our last section we discuss a model which implies that onset of decay would occur later, i.e., $t^*_{reshock} > t^*_{shock}$, because $h_0|_{reshock} > h_0|_{shock}$.

The total mixing widths corresponding to the above four cases are plotted in Fig 2(b) ordered, naturally, by their Δv's. The calculated growth rates are 8.5, 10.8, 17.6, and 22.9 m/s, compared with the experimental values 10.5 ± 0.8, 14.3 ± 1.0, 19.7 ± 1.0, and 23.1 ± 1.0 m/s, respectively. As indicated by the last figure of LMELBSS, the model tends to underestimate the growth rates following weak reshocks, being ~24% below experiment for the worst (EF&C) case, but otherwise is in good agreement with experiments.

IV. ANALYSIS, CONCLUDING REMARKS, AND FUTURE WORK

We have seen that this simple growth and decay model captures well the experimental behavior of *h(t)* under a variety of conditions. Growth following a shock or reshock is given by Eq. (2) and the subsequent decay, after a time t^*, by Eq. (3). The two regimes are joined smoothly, as they must be, by continuity of h and $\dot{h}$. A more complete model would no doubt assure continuity of $\ddot{h}$ also; we hope to pursue such a model in the future. If future work, be it

experimental, numerical or theoretical, reveals that the decay obeys a law different from Eq. (3) then one can always graft it to Eq. (2) in this Fermi-like approach.

After shock and reshock the interface sees a third wave, a rarefaction in the form of acceleration, followed by another period of coasting, a pattern that repeats and gets weaker with time (assuming no new signal coming from the opposite, i.e., driver-section of the shock tube). This third wave is actually an unstable RT acceleration with air "pushing" SF_6 and hence Eq. (1) applies. The acceleration is inversely proportional to the length L of the test section and varies between $\sim 10^5$ m/s^2 ($L = 235$ mm) and $\sim 3\times 10^5$ m/s^2 ($L = 80$ mm). Needless to say, the more complete model would handle shocks, reshocks, accelerations and the in-between coasting periods in one swoop. A possible candidate was the model of Srebrero *et al*,[27] but apparently it does not correctly reproduce h after reshock - see Fig. 8 in LMELBSS. 3D numerical simulations, on the other hand, agree well with the experiments.[18]

Compressibility effects are also neglected in our model, especially upon reshock where it appears most prominently: An instantaneous reduction in $h(t)$ upon reshock. Strictly speaking, one must construct the density profile in the mix region going from pure air to pure SF_6 over a distance of h_- and calculate how that profile steepens upon reshock and yields h_+, the compressed mixing width immediately after reshock. Clearly, it is this h_+ that must be added to Eq. (2) after reshock. Of course $h_+ / h_- \approx 1$ for weak (re)shocks .

A more serious issue, in our opinion, is what to do about $\dot{h}_-$, the growth rate immediately before reshock. In the experiments so far reshock has occurred after decay and, as mentioned earlier, $\dot{h}$ decays almost to zero before being revived by the reshock, hence this is not an urgent issue: $\dot{h}_+ = 2\alpha A \Delta v >> \dot{h}_-$. The question becomes important, at least conceptually, for the opposite

case: What if a *strong* shock is followed by a weak reshock? Surely the growth rate does not immediately drop to zero and $\dot{h}_-$ must then be taken into account.

The question under consideration, whether $\dot{h}_-$ should be added to or subtracted from $2\alpha A\Delta v$, must be answered by that elusive complete model for turbulent mix. It is quite possible that this weakness of our model where we ignore $\dot{h}_-$, justified on the basis that $\dot{h}_- << \dot{h}_+$, is responsible for the poor performance noted earlier when the shocks or reshocks are weak. Referring to Fig. 2, it is clear that cases A and B are most susceptible to this issue and they indeed compare poorly with experiment.

Finally, we discuss t^*. It is straightforward to determine t^* experimentally or phenomenologically as we have done: Fit a shock- or reshock-induced mixing width using Eq. (2) followed by Eq. (3) at $t = t^*$. Note that t^* is the only "free parameter" at our disposal because α^b, α^s, θ^b, and θ^s are all predetermined by RT experiments.

As far as we know all turbulence models attempting to describe RT or RM mix have at least one, and often more than one, free parameter. Examples can be found in Refs. 27 and 28. In particular KL or $k-\varepsilon$ models where $K = k \equiv$ turbulent kinetic energy, $L \equiv$ turbulent-mixing-length-scale [not to be confused with test-section-length!], and $\varepsilon \equiv$ dissipation require an initial nonzero value L_0 or ε_0 because, with $K_0 = k_0 = 0$, naturally no turbulence and no mix develops if L_0 or $\varepsilon_0 = 0$ also – one needs a "seed" that can be amplified by a shock or acceleration. In contrast, we take $h_0 = 0$ and a small h_0, if desired (see below), does not affect our results. In this sense our growth, Eq. (2), is "universal" depending on A and Δv only. But to calculate the subsequent decay, if any, one must decide on t^*, i.e., when decay sets in. It is needed

particularly in long test-section experiments where $\dot{h}$ has time to decay after reshock, as shown in Fig. 1 for $L = 235$ mm.

Needless to say we do not believe that our values for t^* (~0.1 ms for the first shock, ~0.4 ms for the reshock) are universal; Instead, we expect t^* to depend on shock strength Δv and h_0. This follows from a simple dimensional argument: If all that is available is the jump speed Δv (one may also use sound speeds c_s, but they don't help), then no time or length scale can be constructed. In fact this argument is sufficient to pin down the form $h \sim \Delta v t$ for RM just as it does for RT: $h \sim g t^2$. To inject a time scale t^* or length scale h^* one needs an initial length scale, denoted by h_0 for short, because all other length scales are either zero (e.g., shock width) or infinite (e.g., the width of the test section). Therefore,

$$t^* = \frac{h_0}{\Delta v}\beta \tag{6}$$

or, since $h^* = h_0 + 2\alpha A \Delta v t^*$,

$$\frac{h^*}{h_0} = 1 + 2\alpha\beta A, \tag{7}$$

where β is a non-dimensional "constant", possibly a function of A and/or M_s and thus cannot be determined by dimensional arguments.

Assuming β to be a weak function of A, M_s, etc., Eq. (6) implies the following: (1) Stronger shocks with their larger Δv begin to decay earlier, and (2) Interfaces with larger h_0 begin to decay later which is consistent (but certainly no proof) with our using t^*~0.1 ms for the first shock and ~0.4 ms for the reshock. Clearly, an experimental scan over M_s, as done in VS

and LMELBSS, would settle the issue, but of course one must somehow eliminate the effect of the membrane and use a long shock tube.

Equation (7) states that decay begins after the mixing width has grown to $1+2\alpha\beta A$ times its initial value. Let us concentrate on the reshock in the long (235 mm) shock tube experiment displayed in Fig. 1: The reshock induces h to grow from 6.2 mm to 15.3 mm before it begins to decay, 0.4 ms after reshock. Therefore $h_0 = 6.2$ mm, $h^* = 15.3$ mm, and $t^* = 0.4$ ms. From Eq. (6), using $\Delta v = 93.6$ m/s, we obtain $\beta = \Delta v t^* / h_0 \approx 6$ and, from Eq. (7), we obtain $h^*/h_0 = 1+2\alpha\beta A \approx 1+0.34*6*0.72 \approx 2.5$.

An extremely powerful assumption, not justified by any data simply because this issue has not been attacked previously, is to take β to be a constant. If this is true, then all the A-dependence is explicitly indicated in Eq. (7), remembering that $\alpha = \alpha^b + \alpha^s$ and while α^b appears to be constant α^s depends on A. We have seen that A changes little under shock or reshock in the LMELBSS experiments, and therefore $h^*/h_0 \approx 2.5$ for all Δv when $A \sim 0.7$. For other experiments one needs only their Atwood number to evaluate Eq. (7). Armed with this result we can return to the first shocks in Fig. 1, starting with $M_s = 1.20$. As mentioned, we took $t^* = 0.1$ ms which implies $h^* = 1.6$ mm; consequently, $h_0 = h(t=0) = 1.6/2.5 \approx 0.64$ mm. Adding this small value to the curves in Fig. 1 or Fig. 2(b) will not affect any conclusion.

Similarly for the $M_s = 1.33$ shock: For consistency, we take $h_0 = 0.64$ mm (same interface, stronger shock) and $t^* = 0.06$ ms ($0.1 \times 69.1/108.6$) instead of the 0.1 ms assumed in Fig. 1. With this finite h_0 but shorter t^* one finds that h^{b+s} grows only to ~5.4 mm (instead of 6.4 mm) before reshock and to 16.1 mm (instead of 17.1 mm) at the end of the run. Clearly, the 1

mm difference is too small to differentiate experimentally. New experiments focusing on the relationship between h_0 (initial conditions) and t^* (onset of decay) are needed to determine if β depends on A, M_s, etc., or is truly a constant ≈ 6.

For a constant β Eq. (7) reaches its maximum when $A=1$. If $\alpha^s(A=1) \approx 2.5\alpha^b$, as in Ref. 19, then $2\alpha = 2(\alpha^b + \alpha^s) \approx 7\alpha^b \approx 0.42$, hence $(h^*/h_0)_{\max} = 1+2\alpha\beta \approx 1+2.5 = 3.5$. There is clearly much to be done to explore the idea of a t^* or h^* which, as far as we know, has not been previously considered for turbulent mix.

We close by proposing a possible understanding of t^* in response to the natural question: What triggers the decay? Eq. (2) is growth linear in time, $h \sim t$. A well-known alternative, based on conservation of energy and a simple dimensional argument due to Barenblatt[29] gives $h \sim t^{2/3}$ as the evolution of a turbulent layer initially very thin. In discussing that result we proposed[30] that the *nonisotropic* nature of a shock allows one to sidestep Barenblatt's iron-clad argument. We believe it is the *loss* of this anisotropy, i.e. return to isotropic turbulence, that is signaled by t^* – sometime after the passage of the shock the mixing layer "forgets" the direction of the shock and begins to evolve more or less isotropically. In contrast to the commonly held view that "RM turbulence remembers its initial conditions," we claim that "RM forgets the direction of the shock." When this happens, the evolution passes from a linear t to a t^θ behavior signifying essentially the decay of isotropic, homogeneous turbulence.

Compare with RT turbulence: There is no loss of memory of the direction of the acceleration and therefore Eq. (1) holds and there is no second regime as long as $\vec{g} = const$. Again, it is thought that RT turbulence is well at hand because it is independent of initial conditions while RM mixing is "difficult" because it remembers the initial conditions. We agree

that RM is difficult but for the opposite reason: It forgets the direction of the shock and transitions to decaying, isotropic, homogeneous turbulence, hence a second regime. If this hypothesis is correct then mix models must be radically modified because they contain no mechanism for losing memory of a direction. We hope experiments will be carried out with a view towards verifying or falsifying such a hypothesis.

REFERENCES

[1]Lord Rayleigh, *Scientific Papers*, **2**, (Dover, New York, 1965).

[2]G. I. Taylor, "The instability of liquid surfaces when accelerated in a direction perpendicular to their planes, I," Proc. R. Soc. London Ser. A **201**, 192 (1950).

[3]R. D. Richtmyer, "Taylor instability in shock acceleration of compressible fluids," Commun. Pure Appl. Math. **13**, 297 (1960).

[4]E. E. Meshkov, "Instability of the interface of two gases accelerated by a shock wave," Fluid Dyn. **4**, 101 (1969).

[5]J. H. Nuckolls, L. Wood, A. Thiessen, and G. B. Zimmerman, "Laser compression of matter to super-high densities: thermonuclear (CTR) applications," Nature **239**, 139 (1972).

[6]J. D. Lindl, *Inertial Confinement Fusion* (Springer, New York, 1998).

[7]D. Arnett, *Supernovae and Nucleosynthesis*, Princeton University Press, Princeton, 1996; B. A. Remington, R. P. Drake, and D. D. Ryutov, "Experimental astrophysics with high power lasers and Z pinches," Rev. Mod. Phys. **78**, 755 (2006).

[8]*Proceedings of the Tenth International Workshop on the Physics of Compressible Turbulent Mixing, Paris, France,* edited by M. Legrand and M. Vandenboomgaerde (Commissariat à

l'Énergie Atomique, Bruyères-le-Châtel, France, 2006); *Proceedings of the 1st International Conference on Turbulent Mixing and Beyond*, Physica Scripta **T132** (2008).

[9]D. Layzer, "On the instability of superposed fluids in a gravitational field," Astrophys. J. **122**, 1 (1955).

[10]K. I. Read, "Experimental investigation of turbulent mixing by Rayleigh-Taylor instability," Physica D **12**, 45 (1984).

[11]D. L. Youngs, "Numerical simulation of turbulent mixing by Rayleigh-Taylor instability," Physica D **12**, 32 (1984).

[12]D. M. Snider and M. J. Andrews, "Rayleigh-Taylor and shear driven mixing with an unstable thermal stratification," Phys. Fluids **6**, 3324 (1994).

[13]G. Dimonte and M. Schneider, "Density ratio dependence of Rayleigh-Taylor mixing for sustained and impulsive acceleration histories," Phys. Fluids **12**, 304 (2000).

[14]G. Dimonte, "Dependence of turbulent Rayleigh-Taylor instability on initial perturbations," Phys. Rev. E **69**, 056305 (2004).

[15]K. O. Mikaelian, "Turbulent mixing generated by Rayleigh-Taylor and Richtmyer-Meshkov instabilities," Physica D **36**, 343 (1989).

[16]M. Vetter and B. Sturtevant, "Experiments on the Richtmyer-Meshkov instability of an air/SF_6 interface," Shock Waves **4**, 247 (1995).

[17]L. Erez, O. Sadot, D. Oron, G. Erez, L. A. Levin, D. Shvarts, and G. Ben-Dor, "Study of the membrane effect on turbulent mixing measurements in shock tubes," Shock Waves **10**, 241 (2000).

[18]E. Leinov, G. Malamud, Y. Elbaz, L. A. Levin, G. Ben-Dor, D. Shvarts, and O. Sadot, "Experimental and numerical investigation of the Richtmyer-Meshkov instability under re-shock conditions," J. Fl. Mech. **626**, 449 (2009).

[19]HH. Shi, G. Zhang, K. Du, and HX. Jia, "Experimental study on the mechanism of the Richtmyer-Meshkov instability at a gas-liquid interface," J. Hydrodynamics **21**, 423 (2009).

[20]R. E. Tipton, in *Megagauss Technology and Pulsed Power Applications*, edited by C. M. Fowler, R. S. Caird, and D. J. Erickson (Plenum, New York, 1987); R. T. Barton, in *Numerical Astrophysics*, edited by J. M. Centrella, J. M. LeBlanc, R. L. Bowers, and J. A. Wheeler (Jones and Bartlett, Boston, 1985).

[21]U. Alon, J. Hecht, D. Ofer, and D. Shvarts, "Power laws and similarity of Rayleigh-Taylor and Richtmyer-Meshkov mixing fronts at all density ratios," Phys. Rev. Lett. **74**, 534 (1995).

[22]D. Oron, L. Arazi, D. Kartoon, and A. Rikanati, "Dimensionality dependence of the Rayleigh-Taylor and Richtmyer-Meshkov instability late-time scaling laws," Phys. Plasmas **8**, 2883 (2001).

[23]S. Bouquet, P. Gandeboeuf, and P. Pailhoriès, "Analytical study of the buoyancy-drag equation," Math. Meth. Appl. Sci. **30**, 2027 (2007).

[24]K. O. Mikaelian, "Explicit expressions for the evolution of single-mode Rayleigh-Taylor and Richtmyer-Meshkov instabilities at arbitrary Atwood numbers," Phys. Rev. E **67**, 026319 (2003).

[25]R. Courant and K. O. Friedrichs, *Supersonic Flow and Shock Waves* (Springer-Verlag, Berlin, 1948).

[26]K. O. Mikaelian, "Reshocks, rarefactions, and the generalized Layzer model for hydrodynamic instabilities," Phys. Fluids **21**, 024103 (2009).

[27]Y. Srebro, Y. Elbaz, O. Sadot, L. Arazi, and D. Shvarts, "A general drag-buoyancy model for the evolution of the Rayleigh-Taylor and Richtmyer-Meshkov instabilities," Laser Part. Beams **21**, 347 (2003).

[28]G. Dimonte and R. Tipton, "K-L turbulence model for the self-similar growth of the Rayleigh-Taylor and Richtmyer-Meshkov instabilities," Phys. Fluids **18**, 085101 (2006).

[29]G. I. Barenblatt in *Nonlinear Dynamics and Turbulence*, edited by G. I. Barenblatt, G. Iooss, and D. D. Joseph (Pitman, Boston, 1983), p. 48.

[30]K. O. Mikaelian, "Turbulent energy at accelerating and shocked interfaces," Phys. Fluids A **2**, 592 (1990).

This work performed under the auspices of the U.S. Department of Energy by Lawrence Livermore National Laboratory under Contract DE-AC52-07NA27344.

Figure Captions:

Fig. 1. The total mixing width $h^{bubble}+h^{spike}$ in mm versus time in ms for three experiments patterned after the air/SF_6 experiments of LMELBSS.[18] The experiments are labeled by the Mach number M_s of the incoming shock and the length L of the SF_6 test section. We have taken $h_0 = 0$, $t^* = 0.1$ ms for the first shock, and $t^* = 0.4$ ms for the reshock in the 235 mm test section. Variations on h_0 and t^* are discussed in the text. Rigid endwall.

Fig. 2. (a) Air/SF_6 interface velocity in m/s and (b) Total mixing width in mm as functions of time in ms for 4 experiments patterned after LMELBSS[18] who used 4 different endwalls with or without a shock absorber: (A) Elastomeric foam with no cover (most absorptive); (B) Elastomeric foam covered with cardboard (intermediate); (C) Elastomeric foam covered with an aluminum plate (less absorptive); and (D) Fully rigid (no absorption). The shock absorbers which reduce the reshock are modeled as fluids 3, 5, and 40 times heavier than SF_6 for curves A, B, and C, respectively. All have incoming M_s=1.20 and L=80 mm.

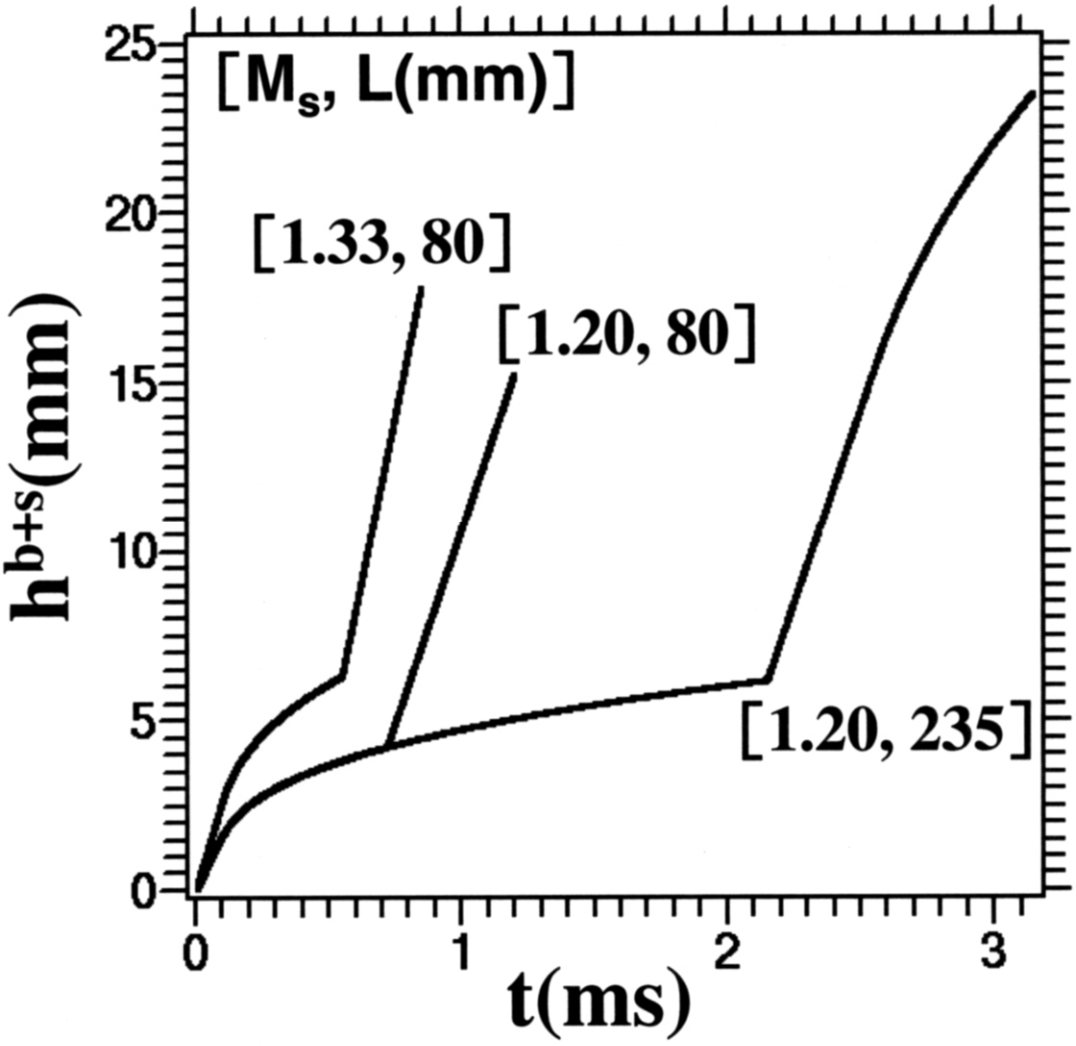

Fig. 1

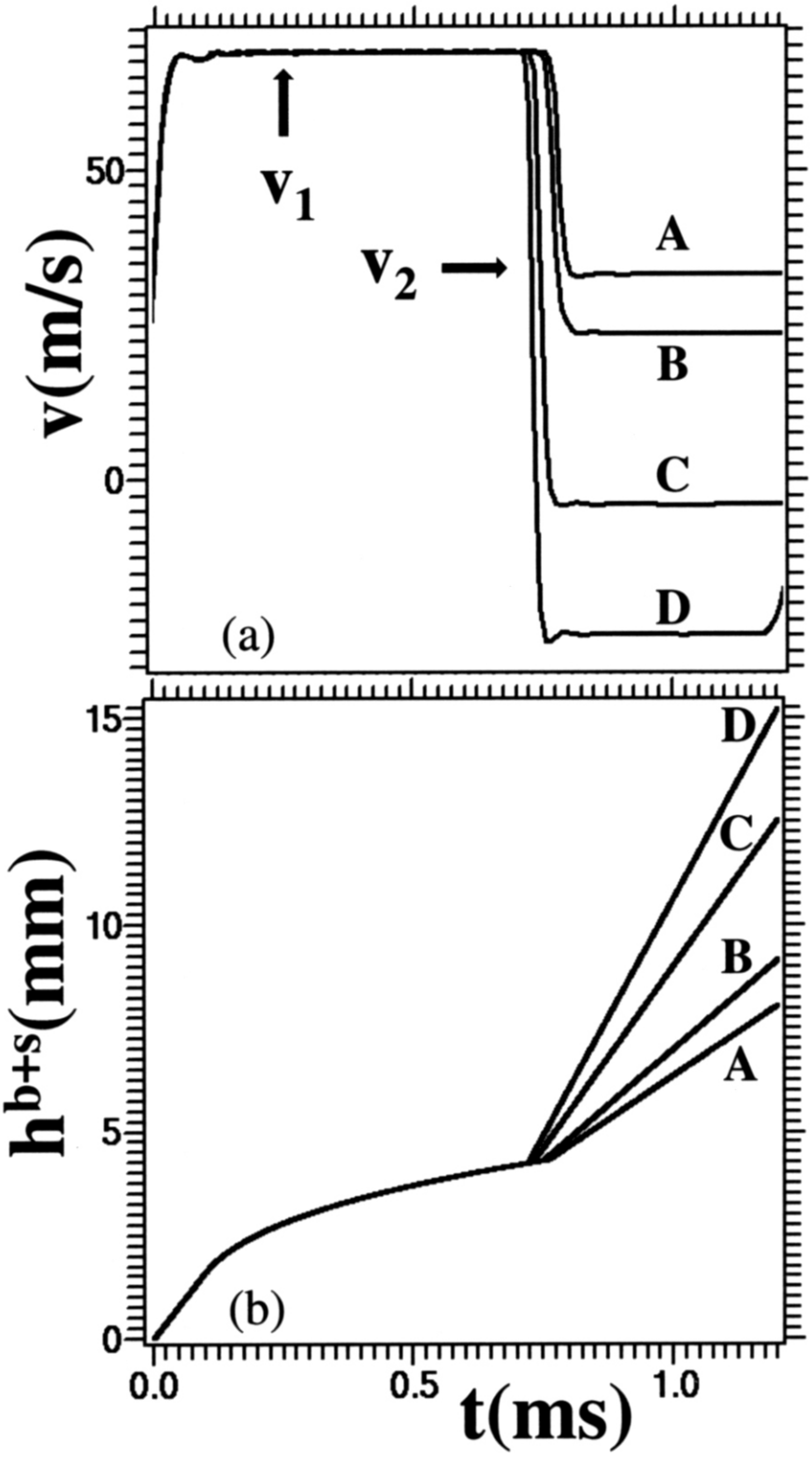

Fig. 2